PNAS
www.pnas.org

Supplementary Information for

TEM1 combinatorially binds to *FLOWERING LOCUS T* and recruits a Polycomb factor to repress the floral transition in Arabidopsis.

Hongmiao Hu[1,2,3,6], Shu Tian[1,3,6], Guohui Xie[2], Rui Liu[2], Nana Wang[2], Sisi Li[2], Yuehui He[1,4,5,7], Jiamu Du[2,7]

[1]National Key Laboratory of Plant Molecular Genetics and Shanghai Center for Plant Stress Biology, Center for Excellence in Molecular Plant Sciences, Chinese Academy of Sciences, Shanghai 201602, China;
[2]Key Laboratory of Molecular Design for Plant Cell Factory of Guangdong Higher Education Institutes, Institute of Plant and Food Science, School of Life Sciences, Southern University of Science and Technology, Shenzhen 518055, China;
[3]University of Chinese Academy of Sciences, Beijing 100049, China
[4]School of Advanced Agricultural Sciences, Peking-Tsinghua Center for Life Sciences, Peking University, Beijing 100871, China
[5]Peking University Institute of Advanced Agricultural Sciences, Weifang, Shandong 261000, China
[6]Co-first authors
[7]Correspondence: Yuehui He, Email: yhhe@pku.edu.cn; Jiamu Du, Email: dujm@sustech.edu.cn.

This PDF file includes:

Supplementary Information Text

SI Materials and Methods

Protein expression and purification

Arabidopsis TEM1-AP2-B3 cassette (residues 50-309), TEM1-AP2 (residues 50-170) and TEM1-B3 (residues 186-309) were cloned into a self-modified pSumo vector with a hexahistidine tag followed by a yeast sumo sequence at the N-terminus of the target protein. The plasmid was transformed into *E. coli* strain BL21(DE3) Rosseta and cultured at 37 °C in LB medium. The protein expression was induced by adding IPTG to a final concentration of 0.2 mM when the OD600 reached 0.7, and the cells were cooled to 16 °C overnight. The recombinant expressed protein was purified using a HisTrap column (GE Healthcare). The hexahistidine plus yeast sumo tag was removed by ulp1 protease digestion followed by a second step HisTrap column (GE Healthcare). The target protein was further purified using Heparin and Superdex G75 columns (GE Healthcare). All oligos were purchased from Sangon Biotech (Shanghai) (Table S1).

Crystallization and structure determination

All DNA segments are derived from the TEM1 recognition sequence in the *FT* 5'-UTR region. An 11-bp DNA segment with 3'-G/C overhangs (Table S1) was used for AP2 domain crystallization. A 14-bp DNA segment with 5'-G/C overhangs (Table S1) was used for B3 domain crystallization. Forward and reverse DNA strands were annealed together and mixed with the purified proteins with a molar ratio of 1.1:1. The crystal screening was carried out using hanging-drop vapor diffusion method at 20 °C. Crystal of TEM1 AP2 was grown under the condition of 0.2 M Li_2SO_4, 0.1 M Tris pH 8.5, 18% PEG 8,000. Crystal of TEM1 AP2-DNA was grown under the condition of 0.2 M NH_4Cl, 0.1 M NaAc, pH 5.0, 20% PEG 6,000. Crystal of TEM1 B3-DNA was grown under the condition of 0.1 M MgAc, 0.1 M MES, pH 6.5, 10% PEG 10,000. The crystals were cryo-protected into reservoir solution supplemented with 20% glycerol and flash cooled into liquid nitrogen. All data were collected in Shanghai Synchrotron Radiation Facilities beamline BL19U1 (1) and processed using the program HKL3000 (2). The anisotropy diffraction data of TEM1 B3-DNA were analyzed and corrected by the Diffraction Anisotropy Server (http://services.mbi.ucla.edu/anisoscale/) (3). All the structures were determined using molecular replacement method using the program Phenix (4). TEM1-AP2 apo structure was solved using AtERF1 as model (PDB: 1GCC) (5). TEM1 AP2-DNA was phased using AP2 apo structure as model. TEM1 B3-DNA structure was phased using a predicted model by Robetta web server (http://new.robetta.org/) (6). Models were refined using the program Phenix (4) and were manually built in the program COOT iteratively (7). The structures were finally presented using PyMOL (Schrödinger, Inc.). A summary of the diffraction data collection and structural refinement statistics is listed in Table S2. The sequence alignments were carried out using the program T-Coffee and illustrated using ESPript (8, 9). The protein-DNA interfaces were analyzed by the PISA server (https://www.ebi.ac.uk/pdbe/pisa/) (10).

In vitro protein-DNA binding assay

A 29-bp cognate DNA from the native *FT* 5'-UTR or related mutants (Table S1) were used for the *in vitro* binding assay. Biotinylated forward strand DNA and biotin-free reverse strand were annealed together. The biotinylated dsDNA was subsequently immobilized on a Streptavidin Biosensor (Pall Corporation). The binding was monitored using an Octet RED96 instrument (Pall Corporation) and the data were fitted using the program provided by the instrument manufacturer (Pall Corporation).

Plant materials and growth conditions

The *tem1-1*, *tem1 tem2* mutants have been described previously (11, 12). Plants were grown in long days (16 h light/8 h dark) at around 22 °C under cool white fluorescent light (~90 μmol m^{-2} s^{-1}). Transgenic plants (T_1 generation) were germinated on half-strength MS media supplemented with 22 μg/ml glyphosate /Basta (Yeasen, China) and transferred to soil around three days after germination to score the number of total leaves produced prior to flowering.

Yeast two-hybrid analysis

Referring to the Matchmaker GAL4 Two-Hybrid System (Clontech) manufacturer's instructions, yeast two-hybrid assays were performed to check interactions among proteins in the yeast strain

AH109. Yeast cells growing on synthetic medium without tryptophan (W), leucine (L), histidine (H), and adenine (A) were examined for protein interactions.

Plasmid construction

To create *pTEM1:TEM1*, a 3.9-kb *TEM1* genomic fragment (2.5-kb promoter plus 1-kb genomic coding region additional 0.4-kb downstream sequence) was cloned in the binary vector *pBGW* via Gateway technology (Invitrogen) (13). To generate the *FT* promoter-*GUS* reporter construct, 6.9-kb promoter of *FT* was amplified by PCR from Col-0 genomic DNA, and fused with the 1.8-kb *GUS* coding sequence; subsequently, the *FTpro-GUS* fragment was cloned into the binary vector *pHGW* via Gateway technology (Invitrogen) (13).

ChIP

ChIP assays were conducted using the Magna ChIP kit (Millipore) as described previously with minor modification (14, 15). In brief, total chromatin was extracted from 10-d-old seedlings grown in 1/2 MS plate under long days and subsequently immunoprecipitated with rabbit polyclonal anti-CLF (16) or anti-H3K27me3 (Millipore, 07-449), respectively. To measure the immunoprecipitated fragments of interest, qPCR was conducted on an *ABI QuantStudio6 Flex* real-time PCR system (Applied Biosystems) with iTaq SYBR Green Supermix (Biorad). Each ChIP DNA sample was quantified in triplicate. Primer sequences are described in Table S1.

CoIP

First, *CLF-FLAG* and *HA-TEM1* fusions were generated. To create *p35S:CLF-FLAG*, the whole coding sequence of *CLF* (without the stop codon) was fused in frame with three copies of *FLAG* at 3' end, and the fusion was cloned into the binary vector *pB2GW7* (17) via Gateway technology (Invitrogen). For the generation of *p35S:HA-TEM1*, one copy of *HA* was fused in frame with 5' end of the *TEM1* coding sequence, and further cloned into the binary vector *pMDC32* (18) via Gateway technology (Invitrogen). All resulting constructs were transformed into the *Agrobacterium tumefaciens GV3101* strain. Overnight cultures of *GV3101* carrying *CLF-FLAG* or *HA-TEM1* were spun down and re-suspended in 10 mM MgCl2 to a final OD600 of 0.5; subsequently, these cultures were mixed 1:1 and syringe infiltrated into 3-week-old *N. benthamiana* leaves. After three days, the infiltrated leaves were harvested, and CoIP assays were performed as described previously with minor modifications (19). In brief, total proteins were extracted from *N. benthamiana* leaves expressing *CLF-FLAG*, or *HA-TEM1 /CLF-FLAG* constructs with a lysis buffer (50 mM Tris-HCl, pH 8.0, 150 mM NaCl, 1 mM EDTA, 10% Glycerol, 5 mM DTT, 1 mM PMSF, 0.5% NP-40, 10 mM sodium molybdate, 10 mM sodium fluoride, 2 mM sodium orthovanadate and 1x protease inhibitor cocktail) and then incubated with anti-HA magnetic beads (ThermoFisher, 88836) at 4 °C for about 4 h. The beads were washed five times by the lysis buffer and then boiled in 5x SDS-PAGE loading buffer; subsequently, the proteins were separated in 10% SDS-PAGE gels and blotted to NC membranes (Bio-Rad). Anti-HA (Roche, 3F10) and anti-FLAG antibodies (Sigma, A8592) were used to detect TEM1 and CLF, respectively.

Histological Analysis of β-Glucuronidase (GUS) Staining

According to the previously described protocol (20), 14-day-old T1 seedlings collected at ZT12 under LDs were stained in a 1.5 mM X-Gluc (5-bromo-4-chloro-3-indolyl-β-d-glucuronic acid) solution for 12 h.

RNA analysis

Total RNA was extracted from aerial parts of ~10-day-old seedlings at ZT8 (for *FT* expression) or 14-day-old seedlings expressing *GUS* at ZT12 using the *Eastep Super Total RNA Extraction* kit (Promega) according to the manufacturer's instructions. After reverse transcription, qPCR was performed on an *ABI QuantStudio6 Flex* real-time PCR system using a SYBR Green PCR master mix as previously described (21). The primers for *FT* and *TUB2* amplification have been described previously (22), and listed in Table S1.

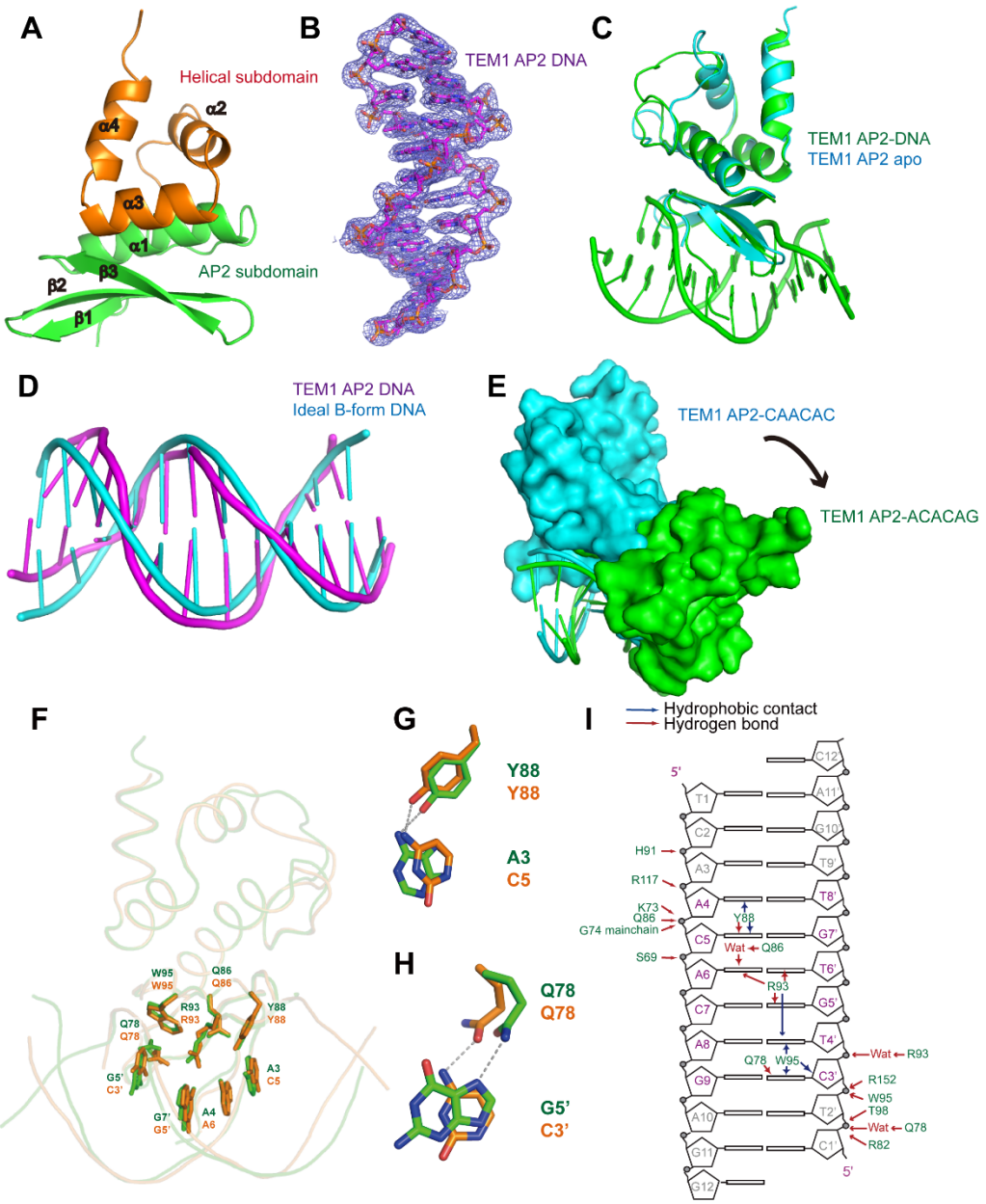

Fig. S1. **TEM1 AP2 structure and DNA density**. (*A*) Crystal structure of TEM1 AP2 with AP2 subdomain depicted in green and helical subdomain depicted in orange. (*B*) SIGMAA weighted 2Fo-Fc map of the DNA in the TEM1 AP2-DNA complex is shown at 1.0 sigma level. (*C*) The superimposition of the structures of TEM1 AP2-DNA complex (in green) and TEM1 AP2 apo structure (in cyan). (*D*) Superposition of DNA in TEM1 AP2-DNA structure (in magenta), with ideal B-form DNA (in cyan). (*E*) The superimposition of AP2-CAACAC (in cyan) and AP2-ACACAG (in green) complex by the position of the DNA showing the AP2 shifting along the DNA major groove by 2-bp with serious steric conflict. (*F*) Superimposition of the AP2-CAACAC (in green) and AP2-ACACAG (in orange) complexes with the base-interacting residues and key bases highlighted in sticks, showing similar protein-base interactions in the two complexes. (*G*) A slightly conformational change of AP2 Tyr88 allows the recognition of A3 and C3 in the two different states. (*H*) A conformational change of Gln78 allows the recognition of G5' and C3' in the two different complexes. (*I*) Schematic representation of the overall interaction between protein and DNA in the AP2-AC<u>ACA</u>G complex.

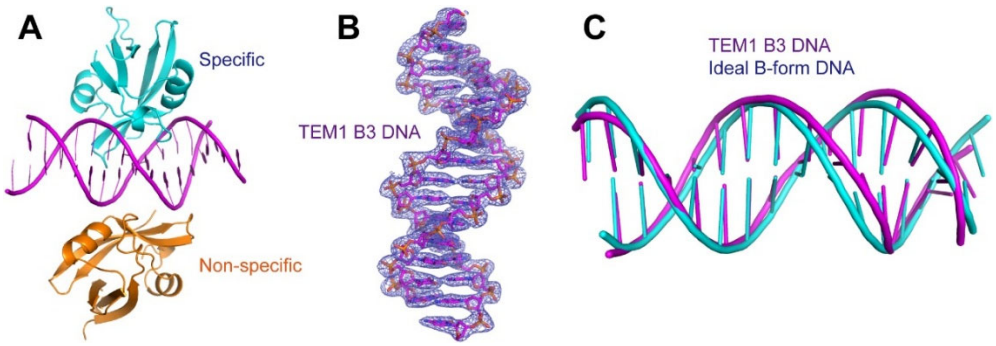

Fig. S2. TEM1 B3 structure and DNA density. (*A*) One asymmetric unit assembly of TEM1 B3-DNA in the crystal possesses two protein and one DNA molecules, with one protein specifically binds to DNA (depicted in cyan), and the other binds non-specially (depicted in orange). (*B*) DNA density of TEM1 B3-DNA complex. SIGMAA weighted 2Fo-Fc map is shown at 1.0 sigma level. (*C*) Superposition of DNA in TEM1 B3-DNA structure in magenta, with ideal B-form DNA in cyan.

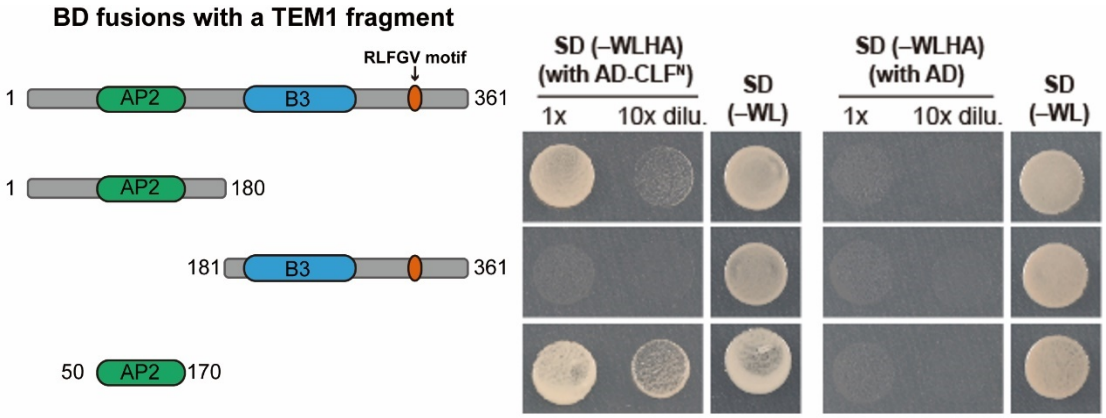

Fig. S3. AP2 domain mediates the interaction of TEM1 with CLF in yeast cells. TEM1 fragments (illustrated on left) and an N-terminal fragment of CLF (aa 1-556) were fused with GAL4-BD and AD domains, respectively. Yeast cells were spotted on selective SD media lacking Trp, Leu, His, and adenine (−WLHA), or a non-selective medium lacking Trp and Leu (−WL; control).

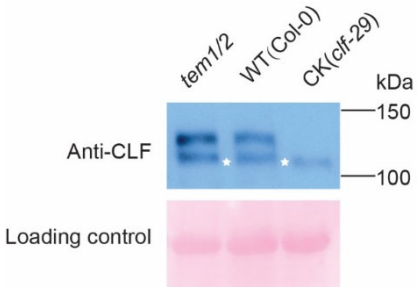

Fig. S4. CLF protein levels in WT and *tem1/2*. Western blotting analysis of CLF abundance in 10-day-old seedlings grown in long days. Total proteins were extracted from *tem1/2* (double mutant), WT, and *clf-29* seedlings, followed by western blotting. The Ponceau S-stained blot serves as the loading control. The asterisk indicates a non-specific band.

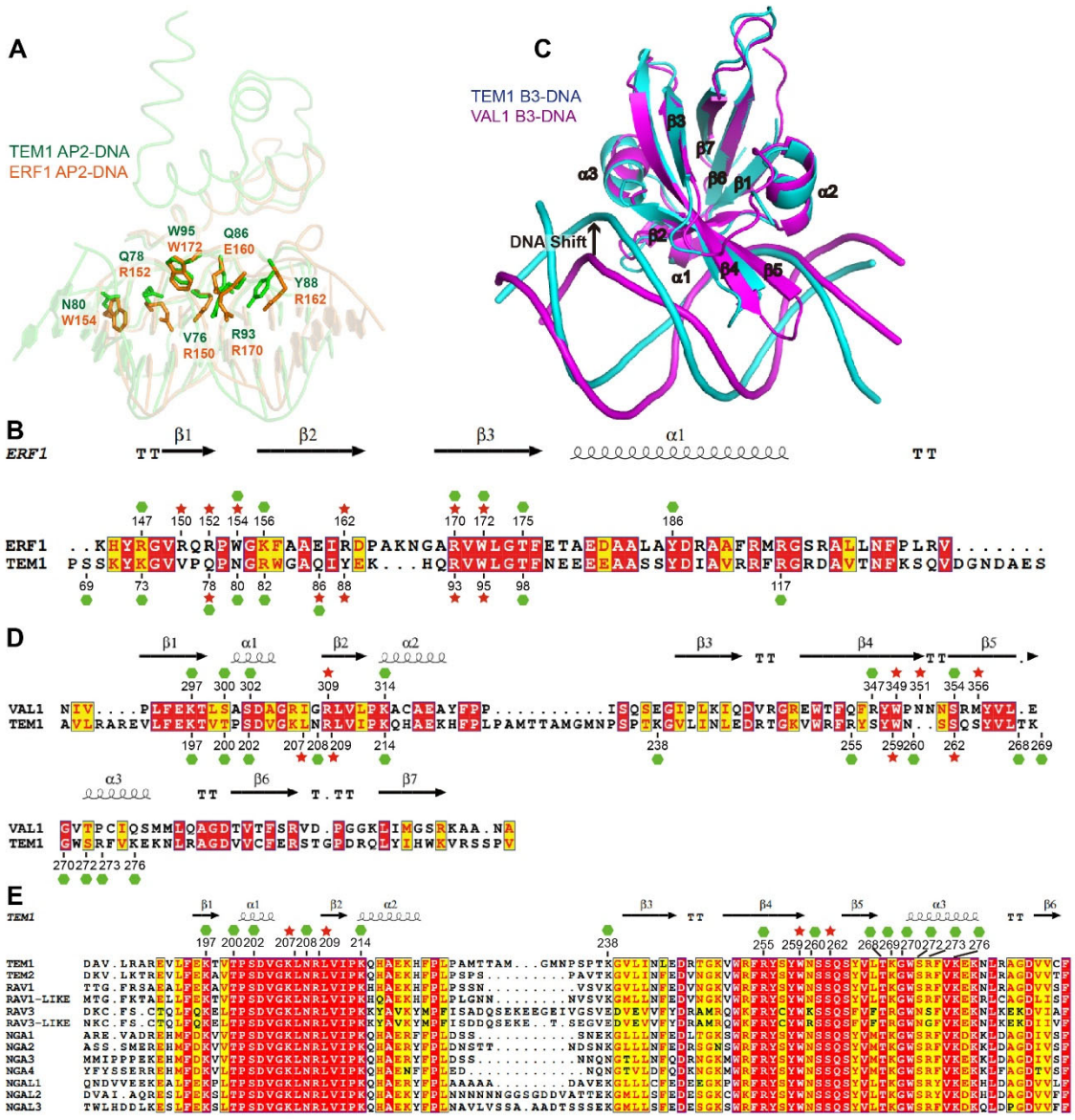

Fig. S5. The structural comparison of AP2 and B3 family proteins, respectively. (*A*) Superimposition of the TEM1 AP2–DNA complex (in green) and ERF1 AP2–DNA complex (PDB: 1GCC, in orange) with the base-interacting residues superimposed and highlighted. (*B*) Structure-based sequence alignment of ERF1 AP2 and TEM1 AP2. The secondary structures of ERF1 and TEM1 are labeled on the top and bottom of the alignment, respectively. The residues involve in DNA base and backbone interactions are marked with red stars and green hexagons, respectively. (*C*) Superimposition of the VAL1 B3–DNA complex (PDB: 6J9A, in magenta) and TEM1 B3-DNA complex (in cyan). Secondary structures are labelled. DNA shift upon TEM1–B3 binding is indicated (arrow). (*D*) Structure-based sequence alignment of VAL1 B3 and TEM1 B3 with their secondary structures labeled on the top and bottom, respectively. The residues contributing to backbone interactions are conserved and marked by green hexagons, while the base interaction residues are diversified and marked by red stars. (*E*) Sequence alignment of TEM1 B3 with other members of RAV subfamily B3 domain. The secondary structure TEM1 B3 is marked on the top of the alignment. The residues involve in DNA base and backbone interactions are marked with red stars and green hexagons, respectively.

Table S1. DNA oligos used in this research. The signature motifs and restriction sites are highlighted by underlines.

Name/Abbreviation	Oligonucleotide sequence	Design purpose
FT-GCC11-3GC	5'- T**CAACA**CAGAG**G** -3'	Crystallization
	5'- CTCTG**TGTTG**A**C** -3'	
FT-RY14-5GC	5'- **G**AAAC**CACCTG**TTTG -3'	Crystallization
	5'- **C**CAAA**CAGGTG**GTTT -3'	
FT 5'-UTR	5'- Biotin-ACAAT**CAACAC**AGAGAAAC**CACCTG**TTTG -3'	BLI
	5'- CAAA**CAGGTG**GTTTCTCT**GTGTTG**ATTGT -3'	
FT-AP2 site 1 mutation	5'- Biotin-A*TTTT***CAACAC***TTTT***AAAC**CACCTG**TTTG -3'	BLI
	5'- CAAA**CAGGTG**GTTT*AAAA***GTGTTG***AAAA*T -3'	
FT-AP2 site 2 mutation	5'- Biotin-ACA*TTTT***ACACAG***TTTT***AC**CACCTG**TTTG -3'	BLI
	5'- CAAA**CAGGTG**GT*AAAA***CTGTGT***AAAA*TGT -3'	
FT-AP2 site 1/2 mutation	5'- Biotin-ACAAT*TTTTTTTT*AGAAAC**CACCTG**TTTG -3'	BLI
	5'- CAAA**CAGGTG**GTTTCT*AAAAAAAA*ATTGT -3'	
TEM1-50-F	5'- CACAGAGAACAGATTGGT**GGATCC**^{BamHI}AGCAGCGTCGTTTTGGATTC -3'	Primer
TEM1-170-R	5'- AGCGGTTTCTTTACCAGA**CTCGAG**^{XhoI}CTAGCCGTTAACAAACTTCCGTC -3'	Primer
TEM1-186-F	5'- CACAGAGAACAGATTGGT**GGATCC**^{BamHI}GCTGTTTTGAGAGCGCGTGA -3'	Primer
TEM1-309-R	5'- AGCGGTTTCTTTACCAGA**CTCGAG**^{XhoI}CTAAACCGGACTAGACCGGACTTTC -3'	Primer
TEM1 S202E 5'	5'- AAGACTGTTACGCCG**GAG**GACGTCGGGA -3'	Primer
TEM1 S202E 3'	5'- **CTC**CGGCGTAACAGTCTTCTCGAACAAA -3'	Primer
TEM1 K214E 5'	5'- CGTTTAGTGATACCG**GAA**CAACACGCGG -3'	Primer
TEM1 K214E 3'	5'- **TTC**CGGTATCACTAAACGGTTCAGCTTC -3'	Primer
TEM1 K238E 5'	5'- AATCCGTCTCCGACG**GAA**GGCGTTTTGA -3'	Primer
TEM1 K238E 3'	5'- **TTC**CGTCGGAGACGGATTCATCCCCATC -3'	Primer
TEM1 R255E 5'	5'- AAAGTGTGGCGGTTC**GAA**TACAGTTACT -3'	Primer
TEM1 R255E 3'	5'- **TTC**GAACCGCCACACTTTCCCTGTTCTA -3'	Primer
TEM1 K269E 5'	5'- AGTTACGTGTTGACC**GAA**GGCTGGAGCC -3'	Primer
TEM1 K269E 3'	5'- **TTC**GGTCAACACGTAACTTTGACTGCTG -3'	Primer
TEM1 K73E 5'	5'- CCTTCGTCGAAATAT**GAA**GGCGTTGTGC -3'	Primer
TEM1 K73E 3'	5'- **TTC**ATATTTCGACGAAGGAAGCTTACGT -3'	Primer
TEM1 Y88E 5'	5'- TGGGGAGCTCAGATT**GAA**GAGAAGCATC -3'	Primer
TEM1 Y88E 3'	5'- **TTC**AATCTGAGCTCCCCATCTTCCGTTA -3'	Primer
TEM1 R93E 5'	5'- TACGAGAAGCATCAG**GAG**GTTTGGCTCG -3'	Primer

TEM1 R93E 3'	5'- **CTC**CTGATGCTTCTCGTAAATCTGAGCT -3'	Primer
TEM1 R117E 5'	5'- GCCGTGAGGAGATTC**GAG**GGCCGCGACG -3'	Primer
TEM1 R117E 3'	5'- **CTC**GAATCTCCTCACGGCGATGTCGTAA -3'	Primer
TEM1 R152E 5'	5'- ATCGTGGATATGTTG**GAG**AAACACACTT -3'	Primer
TEM1 R152E 3'	5'- **CTC**CAACATATCCACGATCTCAGCTTTA -3'	Primer
FT-F	GACCTCAGGAACTTCTATACTTTGGTTATG	RT-qPCR
FT-R	CTGTTTGCCTGCCAAGCTG	RT-qPCR
GUS-F	CTCCTACCGTACCTCGCATTAC	RT-qPCR
GUS-R	ACGCGCTATCAGCTCTTTAATC	RT-qPCR
TUB2-F	GCCTTGTACGATATTTGCTTCAGGAC	RT-qPCR
TUB2-R	CGGAGGTCAGAGTTGAGTTGAC	RT-qPCR
FT-P1F	ACGTTGATGATAGTGAAGTGA	ChIP-qPCR
FT-P1R	ACGCAACCAAGTAGAGACGT	ChIP-qPCR
FT-P2F	ATCCACTTGCCAATCTTCGTAAT	ChIP-qPCR
FT-P2R	TCATTGGTGTAATGACCATGATAAGA	ChIP-qPCR
FT-P3F	TGTGTAGAGGGTTCATGCCTATG	ChIP-qPCR
FT-P3R	ACGTCTCCAACAACTCTGCTTAC	ChIP-qPCR
FT-P4F	CGGTGATGATGCCTATAGTAGTTC	ChIP-qPCR
FT-P4R	CGACTTGGATATTATCAGTACTTTAGTA	ChIP-qPCR
TUB2C-F	ATCCGTGAAGAGTACCCAGAT	ChIP-qPCR
TUB2C-R	AAGAACCATGCACTCATCAGC	ChIP-qPCR

Table S2. Data collection and refinement statistics.

	TEM1 AP2	TEM1 AP2-DNA	TEM1 B3-DNA
Data collection			
Beamline	SSRF-BL19U1	SSRF-BL19U1	SSRF-BL19U1
Space group	$P2_12_12_1$	$P2_12_12$	$P4_322$
PDB code	7ET5	7ET4	7ET6
Wavelength (Å)	0.9792	0.9792	0.9792
Cell dimensions (Å)			
a	37.7	107.3	68.8
b	41.2	135.2	68.8
c	60.0	66.5	163.0
Resolution (Å)	50.0-1.05 (1.09-1.05)[a]	50.0-2.7 (2.80-2.70)	50.0-2.7 (2.80-2.70)
R_{merge}	0.050 (0.791)	0.140 (0.819)	0.061 (0.681)
$I / \sigma I$	24.2 (1.2)	7.4 (1.3)	19.7 (1.6)
Completeness (%)	96.2 (83.0)	99.9 (100.0)	99.1 (99.9)
Redundancy	6.2 (4.9)	4.3 (4.1)	5.6 (5.8)
Refinement			
Resolution (Å) [b]	1.05	2.7	*a**=2.7 *b**=2.7 *c**=2.9
R_{work} / R_{free}	0.164 / 0.174	0.204 / 0.237	0.236 / 0.262
No. reflections	42,669	27,313	10,438
No. atoms	1,700	5,331	2,389
Protein	1,575	3,311	1,757
DNA	-	1,881	609
Solvent	125	139	23
B-factors (Å^2)	20.2	55.1	63.2
Protein	19.7	55.6	65.8
DNA	-	55.2	56.6
Solvent	26.4	39.9	44.9
R.m.s. deviations			
Bond lengths (Å)	0.008	0.005	0.006
Bond angles (°)	0.900	0.970	1.010
Ramachandran plot[c] (%)			
Favored	98.97	98.24	99.01
Allowed	1.03	1.76	0.99
Disallowed, %	0	0	0

[a]Highest-resolution shell is shown in parentheses.
[b]After anisotropic correction, high-resolution data beyond these limits were excluded during refinement. Here, *a**, *b** and *c** denote reciprocal cell directions.
[c]The Ramachandran Plots were monitored using the program MolProbity (23).

SI References

1. Zhang WZ, et al. (2019) The protein complex crystallography beamline (BL19U1) at the Shanghai Synchrotron Radiation Facility. *Nucl Sci Tech* 30(11).
2. Minor W, Cymborowski M, Otwinowski Z, & Chruszcz M (2006) HKL-3000: the integration of data reduction and structure solution--from diffraction images to an initial model in minutes. *Acta Crystallogr D Biol Crystallogr* 62(Pt 8):859-866.
3. Strong M, et al. (2006) Toward the structural genomics of complexes: crystal structure of a PE/PPE protein complex from Mycobacterium tuberculosis. *Proc Natl Acad Sci U S A* 103(21):8060-8065.
4. Adams PD, et al. (2010) PHENIX: a comprehensive Python-based system for macromolecular structure solution. *Acta Crystallogr D Biol Crystallogr* 66(Pt 2):213-221.
5. Allen MD, Yamasaki K, Ohme-Takagi M, Tateno M, & Suzuki M (1998) A novel mode of DNA recognition by a beta-sheet revealed by the solution structure of the GCC-box binding domain in complex with DNA. *EMBO J* 17(18):5484-5496.
6. Yang J, et al. (2020) Improved protein structure prediction using predicted interresidue orientations. *Proc Natl Acad Sci U S A* 117(3):1496-1503.
7. Emsley P, Lohkamp B, Scott WG, & Cowtan K (2010) Features and development of Coot. *Acta Crystallogr D Biol Crystallogr* 66(Pt 4):486-501.
8. Magis C, et al. (2014) T-Coffee: Tree-based consistency objective function for alignment evaluation. *Methods Mol Biol* 1079:117-129.
9. Robert X & Gouet P (2014) Deciphering key features in protein structures with the new ENDscript server. *Nucleic Acids Res* 42(Web Server issue):W320-324.
10. Krissinel E & Henrick K (2007) Inference of macromolecular assemblies from crystalline state. *J Mol Biol* 372(3):774-797.
11. Castillejo C & Pelaz S (2008) The balance between CONSTANS and TEMPRANILLO activities determines FT expression to trigger flowering. *Curr Biol* 18(17):1338-1343.
12. Osnato M, Castillejo C, Matias-Hernandez L, & Pelaz S (2012) TEMPRANILLO genes link photoperiod and gibberellin pathways to control flowering in Arabidopsis. *Nat Commun* 3:808.
13. Karimi M, De Meyer B, & Hilson P (2005) Modular cloning in plant cells. *Trends Plant Sci* 10(3):103-105.
14. Johnson L, Cao X, & Jacobsen S (2002) Interplay between two epigenetic marks. DNA methylation and histone H3 lysine 9 methylation. *Curr Biol* 12(16):1360-1367.
15. Wang Y, Gu X, Yuan W, Schmitz RJ, & He Y (2014) Photoperiodic control of the floral transition through a distinct polycomb repressive complex. *Dev Cel*l 28(6):727-736.
16. Tao Z, et al. (2019) Embryonic resetting of the parental vernalized state by two B3 domain transcription factors in Arabidopsis. *Nat Plants* 5(4):424-435.
17. Karimi M, Inze D, & Depicker A (2002) GATEWAY vectors for Agrobacterium-mediated plant transformation. *Trends Plant Sci* 7(5):193-195.
18. Curtis MD & Grossniklaus U (2003) A gateway cloning vector set for high-throughput functional analysis of genes in planta. *Plant Physiol* 133(2):462-469.
19. Smakowska-Luzan E, et al. (2018) An extracellular network of Arabidopsis leucine-rich repeat receptor kinases. *Nature* 553(7688):342-346.
20. Jiang D, Kong NC, Gu X, Li Z, & He Y (2011) Arabidopsis COMPASS-like complexes mediate histone H3 lysine-4 trimethylation to control floral transition and plant development. *PLoS Genet* 7(3):e1001330.
21. Gu X, Wang Y, & He Y (2013) Photoperiodic regulation of flowering time through periodic histone deacetylation of the florigen gene FT. *PLoS Biol* 11(9):e1001649.
22. Luo X, et al. (2018) The NUCLEAR FACTOR-CONSTANS complex antagonizes Polycomb repression to de-repress FLOWERING LOCUS T expression in response to inductive long days in Arabidopsis. *Plant J* 95(1):17-29.
23. Chen VB, et al. (2010) MolProbity: all-atom structure validation for macromolecular crystallography. *Acta Crystallogr D Biol Crystallogr* 66(Pt 1):12-21.